

# Rethinking Architecture Design for Tackling Data Heterogeneity in Federated Learning

Liangqiong Qu<sup>1\*</sup>, Yuyin Zhou<sup>1\*</sup>, Paul Pu Liang<sup>2\*</sup>, Yingda Xia<sup>3</sup>, Feifei Wang<sup>1</sup>,  
Li Fei-Fei<sup>1</sup>, Ehsan Adeli<sup>1</sup>, Daniel Rubin<sup>1</sup>

<sup>1</sup>Stanford University, <sup>2</sup>Carnegie Mellon University, <sup>3</sup>Johns Hopkins University  
{liangqi, yzhou, ffwang, eadeli, rubin}@stanford.edu, pliang@cs.cmu.edu  
philyingdaxia@gmail.com, feifeili@cs.stanford.edu

## Abstract

Federated learning is an emerging research paradigm enabling collaborative training of machine learning models among different organizations while keeping data private at each institution. Despite recent progress, there remain fundamental challenges such as lack of convergence and potential for catastrophic forgetting in federated learning across real-world heterogeneous devices. In this paper, we demonstrate that attention-based architectures (e.g., Transformers) are fairly robust to distribution shifts and hence improve federated learning over heterogeneous data. Concretely, we conduct the first rigorous empirical investigation of different neural architectures across a range of federated algorithms, real-world benchmarks, and heterogeneous data splits. Our experiments show that simply replacing convolutional networks with Transformers can greatly reduce catastrophic forgetting of previous devices, accelerate convergence, and reach a better global model, especially when dealing with heterogeneous data. We will release our code and pretrained models at <https://github.com/Liangqiong/ViT-FL-main> to encourage future exploration in robust architectures as an alternative to current research efforts on the optimization front.

## 1 Introduction

Federated Learning (FL) is an emerging research paradigm to train machine learning models on private data distributed over multiple heterogeneous devices [43]. FL keeps data on each device private and aims to train a global model that is updated only via communicated parameters instead of the data itself. Therefore, it provides an opportunity for collaborative machine learning across multiple institutions without risking leakage of private data [24, 32, 49]. This has proved especially useful in domains such as healthcare [4, 7], learning from mobile devices [17, 34], smart cities [24], and communication networks [45], where preserving privacy is crucial. Despite the rich opportunities afforded by FL, there remain fundamental research problems to be tackled before FL can be readily applicable to real-world data distributions. Most current methods that aim to learn a single global model across non-IID devices encounter challenges such as non-guaranteed convergence and model weight divergence for parallel FL methods [20, 33, 62], and severe catastrophic forgetting problem for serial FL methods [7, 16, 53].

While most research efforts focus on improving the optimization process in FL, our paper aims to provide a new perspective by rethinking the choice of architectures in federated models. We hypothesize that Transformer architectures [13, 56] are especially suitable for heterogeneous data distributions due to their surprising robustness to distribution shifts [3]. This property has led to the prevalence of Transformers in self-supervised learning where heterogeneity is manifested

\*Equal contribution

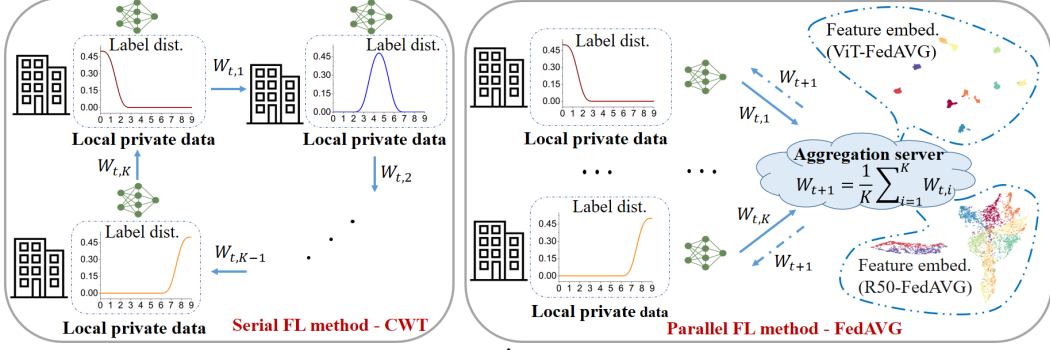


Figure 1: Simplified schematic for a typical serial FL method CWT [7] and a parallel FL method FedAVG [42] on non-IID data partitions of CIFAR-10 [29] with label distribution skewness.  $W_{t,i}$  denotes the model weights during training at round  $t$  on client  $i$  (total  $K$  clients are involved). On the right, we show feature embedding visualizations of ViT-FedAVG and ResNet-FedAVG using UMAP [41]. We find that the features learned by ViT-FedAVG are more clearly separated than those learned by ResNet-FedAVG. Our experiments (section 4.2) support the superiority of ViT-FL on heterogeneous data and we provide empirical analysis explaining their effectiveness (section 4.3)

via distribution shifts between unlabeled pretraining data and labeled test data [12], as well as in multimodal learning over fundamentally heterogeneous input modalities such as image and text [23, 55]. To study this hypothesis, we conduct the first large-scale empirical benchmarking of several neural architectures across a suite of federated algorithms, real-world benchmarks, and heterogeneous data splits. To represent Transformer networks, we use a standard implementation of Vision Transformers [13] on image tasks spanning image classification [29, 36] and medical image classification [26].

Our results suggest that ViT-FL performs especially well in settings with the most heterogeneous device splits, with the gap between ViT-FL and FL with ResNets [18] increasing significantly as heterogeneity increases. To further understand these results, we find that the main source of improvement lies in the increased robustness of Transformer models to heterogeneous data which reduces catastrophic forgetting of previous devices when trained on substantially different new ones. Together, Transformers converge faster and reach a better global model suitable for all devices. By performing comprehensive comparisons to FL methods designed specifically to combat heterogeneous data, we show that ViT-FL provides immediate improvements without using training heuristics, additional hyperparameter tuning, or additional training/fine-tuning. We conclude that Transformer models should be regarded as a natural starting point for FL problems in future research.

## 2 Related Work

**Federated Learning.** Federated learning (FL) aims to train machine learning models on private data across massively distributed devices [43]. To enable effective distributed training across heterogeneous devices, two categories of methods have emerged: (1) parallel FL methods involve training each local client in parallel either synchronously or asynchronously (such as the classic FedAVG [43]), whereas (2) serial methods train each client in a serial and cyclical way (such as Cyclic Weight Transfer (CWT) [7] and Split learning [57]). A schematic description of FedAVG [43] and CWT [7] is illustrated in Figure 1. At its core, FL presents a challenge of data heterogeneity in the distributions of training data across clients, which causes non-guaranteed convergence and model weight divergence for parallel FL methods [20, 33, 62], and severe catastrophic forgetting problem for serial FL methods [7, 16, 53]. Among recent developments to the classic parallel FedAVG algorithm [43] have included using server momentum (FedAVGM) to mitigate per-client distribution shift and imbalance [21], globally sharing small subsets of data among all users (FedAVG-Share) [62], using a proximal term to the local objective (FedProx) to reduce potential weight divergence under severely heterogeneous devices [33], and constructing a shared global model in a layer-wise manner by matching and averaging hidden elements (FedMA) [59].

Concurrently, several recent efforts aim to alleviate catastrophic forgetting in continual and serial learning: constraining the updates on weights that are important to previously seen tasks or clients (elastic weight consolidation (EWC) [28]), applying Deep Generative Replay to mimic data from previous clients or tasks [54], and applying cyclically weighted objectives to mitigate performance loss across label distribution skewness [2], among others. However, all of these approaches mainly focus on improving the optimization algorithm without studying the potential in architecture design to improve robustness to distribution shifts in data. In our work, we show that simple choices in architecture actually make a big difference and should be an active area of study in parallel to the optimization methods that have been the main focus of current work.

**Transformers.** The Transformer architecture was first proposed for sequence-to-sequence machine translation [56] and has subsequently established state-of-the-art performance across many NLP tasks, especially when trained in a self-supervised paradigm [12]. Recently, Transformers have also been found to be broadly applicable to tasks involving images and video. For instance, Parmar *et al.* [46] applied the self-attention in local neighborhoods of an image while the Vision Transformer (ViT) [13] achieved state-of-the-art on ImageNet classification by directly applying Transformers with global self-attention to full-sized images.

Its intriguing performance boosts relative to classical architectures for language (i.e., LSTMs [19]) and vision (i.e., CNNs [18, 31]) have inspired recent interest towards understanding the reasons behind their effectiveness. Among several particularly relevant findings are that ViTs are highly robust to severe occlusions, perturbations, domain shifts [3, 44], as well as synthetic and natural adversarial examples [40, 47]. In addition, recent studies have suggested that Transformers are also suitable for heterogeneous and multimodal data [23, 37, 55]. Inspired by these findings, we hypothesize that ViTs will also be highly effective in adapting to data heterogeneity in FL, and provide detailed empirical analysis to test this hypothesis.

### 3 Transformers in Federated Learning

In this section, we present background on Transformer architectures and federated learning methods.

#### 3.1 Vision Architectures

**CNN.** For convolution-based architectures, we use ResNet-50 [18], which contains a sequence of convolution, ReLU, pooling, and batch normalization layers. ResNet-50 is among the most popular architectures for image classification and has been the standard architecture used in FL on image data [1, 35].

**Transformers.** As a comparison, we employ Vision Transformers (ViT) [13], which do not use conventional convolution layers. Instead, the image features are extracted in the following two steps:

- **Image Sequentialization.** Following [13], we first perform tokenization by reshaping the input  $\mathbf{x}$  into a sequence of flattened 2D patches  $\{\mathbf{x}_p^i \in \mathbb{R}^{P^2 \cdot C} | i = 1, \dots, N\}$ , where each patch is of size  $P \times P$  and  $N = \frac{HW}{P^2}$  is the number of image patches (i.e., the input sequence length).
- **Patch Embedding.** We map the vectorized patches  $\mathbf{x}_p$  into a latent  $D$ -dimensional embedding space using a trainable linear projection. To encode spatial information, we learn specific position embeddings which are added to the patch embeddings to retain positional information as follows.

$$\mathbf{z}_0 = [\mathbf{x}_{class}; \mathbf{x}_p^1 \mathbf{E}; \mathbf{x}_p^2 \mathbf{E}; \dots; \mathbf{x}_p^N \mathbf{E}] + \mathbf{E}_{pos}, \quad (1)$$

where  $\mathbf{x}_{class}$  stands for the class token.  $\mathbf{E} \in \mathbb{R}^{(P^2 \cdot C) \times D}$  and  $\mathbf{E}_{pos} \in \mathbb{R}^{N \times D}$  denote the patch embedding projection the position embedding respectively. The Transformer encoder consists of  $L$  layers of Multi-head Self-Attention (MSA) and Multi-Layer Perceptron (MLP) blocks (Eq. (2)(3)). Therefore the output of the  $\ell$ -th layer can be written as follows:

$$\mathbf{z}'_\ell = \text{MSA}(\text{LN}(\mathbf{z}_{\ell-1})) + \mathbf{z}_{\ell-1}, \quad (2)$$

$$\mathbf{z}_\ell = \text{MLP}(\text{LN}(\mathbf{z}'_\ell)) + \mathbf{z}'_\ell, \quad (3)$$

where  $\text{LN}(\cdot)$  denotes the layer normalization operator and the first element of the  $L$ -th layer output  $\mathbf{z}_L^0$  is the corresponding image representation  $\mathbf{y}$ .

**Hybrid Model.** Finally, we also experiment with the CNN-Transformer hybrid (ViT-H) model as proposed in [13] where ResNet-50 (GN) is first used as a feature extractor to generate a feature map

for the input. GN here indicates replacing all Batch normalization layers in ResNet-50 with Group Normalization. The patch embedding is applied to  $1 \times 1$  patches extracted from the CNN feature map instead of from raw images.

### 3.2 Federated Learning Methods

We apply one of the most popular parallel methods (FedAVG [43]) and serial methods (CWT [7]) as training algorithms (see schematic descriptions in Figure 1).

**Federated Averaging.** FedAVG combines local stochastic gradient descent (SGD) on each client with iterative model averaging [43]. Specifically, a fraction of local clients are randomly sampled in each communication round, and the server sends the current global model to each of these clients. Each selected client then performs  $E$  epochs of local SGD on its local training data and sends the local gradients back to the central server for aggregation synchronously. The server then applies the averaged gradients to update its global model, and the process repeats.

**Cyclic Weight Transfer.** In contrast to FedAVG where each local client is trained in a synchronous and parallel way, the local clients in CWT are trained in a serial and cyclic way. In each round of training, CWT trains a global model on one local client with its local data for a number of epochs  $E$ , and then cyclically transfers this global model to the next client for training, until all the local clients have been trained on once [7]. The training process then cycles through the clients repeatedly until the model converges or a predefined number of communication rounds is reached.

## 4 Experiments

Our experiments are designed to answer the following research questions that are of importance to practical deployment of FL methods, while also aiding our understanding of (vision) Transformer architectures.

- Are Transformers able to learn a better global model in FL settings as compared to CNNs which have been the de-facto approach on FL tasks (section 4.2)?
- Are Transformers especially capable of handling heterogeneous data partitions (section 4.3.1)?
- Do Transformers reduce communication costs as compared to CNNs (section 4.3.2)?
- What are practical tips helpful for practitioners to deploy Transformers in FL (section 4.4)?

Experimental code is included in the supplement and will be made public after blind review.

### 4.1 Experimental Setup

Following [7, 20], we evaluate different FL methods on the Kaggle Diabetic Retinopathy competition dataset (denoted as Retina) [26] and CIFAR-10 dataset [29] in our study. Specifically, we binarize the labels in the Retina dataset to Healthy (positive) and Diseased (negative), randomly selecting 6,000 balanced images for training, 3,000 images as the global validation dataset, and 3,000 images as the global testing dataset following [7]. We use the original test set in CIFAR-10 as the global test dataset, set aside 5,000 images from the original training dataset as the global validation dataset, and use the remaining 45,000 images as the training dataset. Detailed image pre-processing steps for Retina and CIFAR-10 dataset are shown in Appendix A.1. We simulate three sets of data partitions for both Retina and CIFAR-10: one IID-data partition, and two non-IID data partitions with label distribution skew. Each data partition in Retina and CIFAR-10 dataset contains 4 and 5 simulated clients, respectively. We use the mean Kolmogorov-Smirnov (KS) statistics between every two clients to measure the degree of label distribution skewness.  $KS = 0$  indicates IID data partitions, while  $KS = 1$  results in an extremely non-IID data partition. The detailed data partitions are shown in Appendix A.1.

We use linear learning rate warm-up and decay scheduler for ViT-FL. The learning rate scheduler for FL with CNNs is selected from linear warm-up and decay or step decay. Gradient clipping (at global norm 1) is applied to stabilize the training. We set local training epoch in all the FL methods to 1, and the total communication round to 100, unless otherwise stated. More implementation details are shown in Appendix A.2.

	Central	Split-1, KS-0	Split-2, KS-0.49	Split-3, KS-0.57
R50-CWT	81.60	81.97	78.43	73.88
ViT-CWT	80.16	79.22 $\downarrow$ 2.75	78.68 $\uparrow$ 0.25	78.02 $\uparrow$ 4.20
ViT-H-CWT	81.77	82.10 $\uparrow$ 0.13	80.57 $\uparrow$ 2.14	80.58 $\uparrow$ 6.70
R50-FedAVG	81.60	80.48	75.96	75.76
ViT-FedAVG	80.16	80.36 $\downarrow$ 0.12	78.33 $\uparrow$ 2.37	78.13 $\uparrow$ 2.37
ViT-H-FedAVG	81.77	83.00 $\uparrow$ 1.92	81.53 $\uparrow$ 4.17	81.20 $\uparrow$ 4.81

Table 1: Prediction accuracy (%) on Retina dataset. The arrows indicate the changes in performance w.r.t. the ResNet counterparts. Vision Transformers (both ViT and ViT-H) show consistently strong performance especially in non-IID data partitions.

	Central	Split-1, KS-0	Split-2, KS-0.65	Split-3, KS-1
R50-CWT	96.27	96.48	70.58	20.23
ViT-CWT	98.60	98.93 $\uparrow$ 2.45	98.88 $\uparrow$ 28.30	98.02 $\uparrow$ 77.79
ViT-H-CWT	98.24	98.86 $\uparrow$ 2.38	98.78 $\uparrow$ 28.20	98.06 $\uparrow$ 77.83
R50-FedAVG	96.27	96.75	93.06	60.79
ViT-FedAVG	98.60	99.02 $\uparrow$ 2.26	98.81 $\uparrow$ 5.75	98.14 $\uparrow$ 37.35
ViT-H-FedAVG	98.24	98.83 $\uparrow$ 2.07	98.50 $\uparrow$ 5.44	97.56 $\uparrow$ 36.77

Table 2: Prediction accuracy (%) on CIFAR-10 dataset. The arrows indicate the changes in performance w.r.t. the ResNet counterparts. Vision Transformers (both ViT and ViT-H) show consistently strong performance in both IID and non-IID data partitions, with especially significant improvements on the most heterogeneous split (Split-3).

## 4.2 Results

**Comparison of FL with different neural architectures and (ideal) centralized training:** Both CWT and FedAVG achieve comparable results to a model trained on centrally hosted data (denoted as Central) on the IID setting no matter which architecture (R-50, ViT, and ViT-H) is applied as the backbone network (Table 1 and Table 2). However, we observe a significant reduction in test accuracy for R50-CWT and R50-FedAVG on heterogeneous data partitions, especially on extremely heterogeneous data partitions (Split 3, KS-1 of CIFAR-10). By simply replacing ResNet-50 with ViT (or ViT-H), both CWT and FedAVG successfully retain model accuracy even in highly heterogeneous non-IID settings. In particular, ViT-CWT and ViT-FedAVG improve the test accuracy relative to R50-CWT and R50-FedAVG by 77.79% and 37.35% on the highly heterogeneous Split-3, KS-1 of CIFAR-10 dataset. Therefore, ViT is particularly suitable for heterogeneous data in FL.

**Comparison with existing FL methods:** We also compare ViT-FL to several state-of-the-art optimization based FL methods: FedAVGM [21], FedProx [33], and FedAVG-Share [61]. We use ResNet-50 as the backbone network for all the compared FL methods. We tune the best parameters (including learning rate, momentum parameter  $\beta$  for FedAVGM, and penalty constant  $\mu$  in the proximal term of FedProx) on Split-2 dataset with grid search, and apply the same parameters to all the remaining data partitions. We allow each client to share 5% percentage of their data among each other for FedAVG-Share.

As shown in Figure 2, ViT-FL noticeably outperforms all the other FL methods in non-IID data partitions. Both FedProx [33] and FedAVGM [21] suffer severe performance drops on highly heterogeneous data partitions despite carefully tuned optimization parameters. Similarly, FedAVG-Share also suffers from performance drops on highly heterogeneous data partition Split-3 even when 5% percentage of the local data is shared among all clients (94.4% of Split-3 on CIFAR-10 dataset compared to 97% on Split-1). We conclude that simply using Transformers can improve upon several recent methods designed for federated optimization, which often require careful tuning of optimization parameters.

## 4.3 Analyzing the Effectiveness of Transformers

Given these promising empirical results on a suite of FL benchmarks and in comparison with state-of-the-art FL methods, we now perform a careful empirical analysis to uncover what exactly contributes to Transformers’ improved performance.

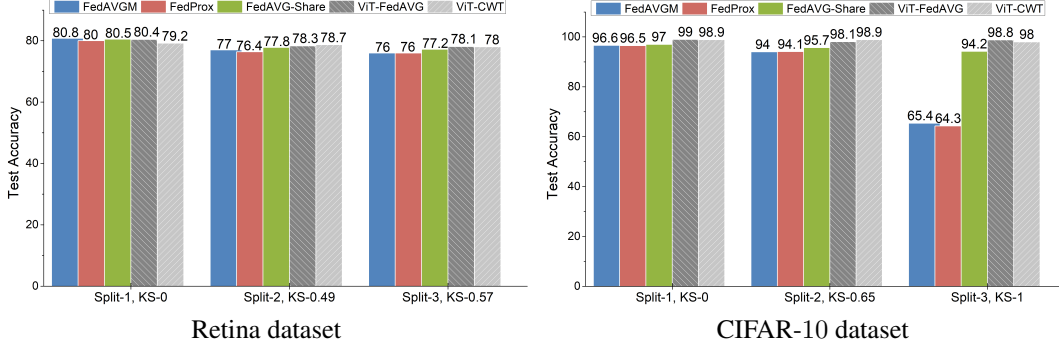


Figure 2: Comparisons with state-of-the-art optimization based federated learning methods with ResNet-50 as backbone. Vision Transformer-based FL methods (ViT-CWT and ViT-FedAVG) outperform other methods in non-IID data partitions.

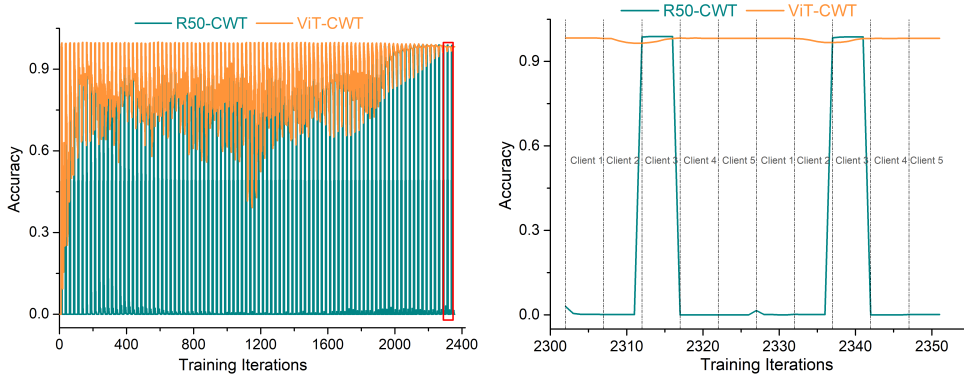


Figure 3: Left: evolution of the prediction accuracy on the validation dataset of client 3 (which shares the same data distribution as its local training dataset) as more clients are involved in CWT learning on Split 3 of CIFAR-10 dataset. Right: zoom in on the red rectangular in the left image. The training order of different clients is also shown. The sequential training strategy of R50-CWT always incurs catastrophic forgetting on the previous clients under highly heterogeneous data distributions. ViT-CWT helps alleviate this problem due to its strong generalization ability.

#### 4.3.1 Transformers Generalize Better in the non-IID Setting

The distributed nature of FL means that there can be substantial heterogeneity in data distributions across clients. Prior research has shown that training FL models with FedAVG or CWT incurs issues such as weight divergence and catastrophic forgetting respectively [28, 53]. We argue that the local convolutions used in CNNs, which have been shown to rely more on local high-frequency patterns [15, 25, 58], might be particularly sensitive to heterogeneous devices. This problem is particularly prevalent in FL over healthcare data since input images captured by different institutions may vary significantly in local patterns (difference in intensity, contrast, etc.) due to different medical imaging protocols [16, 50], as well as in natural data splits across users due to user idiosyncrasies in speaking [30], typing [17], and writing [27]. On the other hand, ViTs have been shown to be significantly less biased towards local patterns as compared to CNNs and instead use self-attention to learn global interactions [48], which may contribute to their surprising robustness to distribution shifts and adversarial perturbations [3, 44]. To provide a deeper analysis of the generalization capabilities of Transformers across heterogeneous data, we design the following two empirical experiments:

**Catastrophic forgetting across heterogeneous devices:** The model learned with CNNs often works worse on out-of-distribution data. This phenomenon is especially severe in the serial FL method CWT. Due to its sequential and serial training strategy, training CNNs in a CWT paradigm usually results in catastrophic forgetting on non-IID data partitions: the model’s performance on previous clients abruptly degrades after a few updates on a new client with a different data distribution [3, 44].

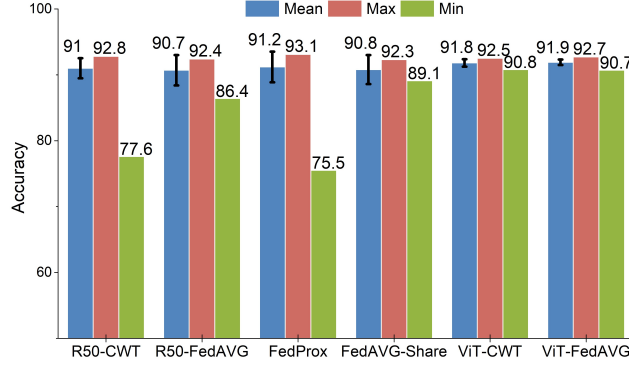


Figure 4: Prediction accuracy (%) of models on the global test dataset (union of the test data from all local clients) of CelebA [36]. The mean (w/ standard deviation), maximum, and minimum test accuracies are reported here. Note that the prediction accuracies for centralized training with ResNet and ViT are 91.89 and 91.17, respectively. Vision Transformer-based FL methods (ViT-CWT and ViT-FedAVG) consistently outperform the other approaches while also reducing variance.

This results in poorer and slower convergence which is undesirable in FL. Similar forgetting issues have also been found in the transfer learning literature [8, 11, 52].

We evaluate CWT on Split-3 of the CIFAR-10 dataset to show this catastrophic forgetting phenomenon. In Figure 3, we plot the evolution of the prediction accuracy on the validation dataset of Client-3 (which shares the same data distribution as its training dataset) as more clients are involved in CWT learning. When transferring a well-trained model on Client-3 to Client-4, the prediction accuracy on the previous Client-3 validation dataset degrades abruptly and dramatically (from  $> 98\%$  to  $< 1\%$  accuracy). However, the model trained with ViT as backbone (ViT-CWT) is able to transfer knowledge from Client-3 to Client-4 while losing only small amounts of information on Client-3 (maintains accuracy at  $98\%$ ). Therefore, ViTs generalize better to new data distributions without forgetting old ones. Please refer to Appendix B.1 for additional analysis on catastrophic forgetting.

**Generalization of ViT-FL on real-world federated datasets:** A well-trained federated model should perform well on out-of-distribution test datasets of other unseen clients. To test the generalizability of Transformers, we further apply it to a real-world federated CelebA dataset [36] and compare it to the ResNet counterparts, FedProx [33], and FedAVG-Share [61]. CelebA is a large-scale face attributes dataset with more than 200K celebrity images and is participated by the celebrity on the image. We use a specially designed federated version of CelebA provided by the LEAF benchmark [5] which partitions into devices based on the celebrity in the picture. Following [5], we test on the binary classification task (presence of smile), drop clients with fewer than 10 samples, and use 5% of the total clients for training. This results in a total of 429 clients each with an average of  $22.6 \pm 6.23$  samples and a total of 9704 samples.

We report the mean (with standard deviation), maximum, and minimum test accuracies of models trained using different FL methods on the union of the test data from all local clients in Figure 4. Our ViT-FL approach ( $91.8 \pm 0.57\%$  for ViT-CWT and  $91.9 \pm 0.42\%$  for ViT-FedAVG) achieves comparable performance to the centralized training (91.17%), outperforms state-of-the-art FL methods, and also shows much smaller standard deviation in results. With ResNet-50, while some clients achieve promising performance on the test dataset of other clients, there still remain some clients that suffer (e.g., maximum accuracy of FedProx is 93.1% but minimum accuracy drops to 75.5%). Globally sharing 5% of data among all clients in FedAVG-Share helps improve generalization, but it still shows a larger deviation from the mean ( $90.8 \pm 2.21$ ). In contrast, models trained under ViT-FL show consistently strong performance across all clients with low variance. This again shows that Transformers learn a better global model than their CNNs counterparts.

#### 4.3.2 Transformers Converge Faster and to Better Optimum

A powerful FL method should not only perform robustly on both IID and non-IID data partitions but also have low communication costs to enable deployment over communicated-limited bandwidths. Communication cost is determined by the number of communication rounds till convergence and the number of communication parameters (typically model parameters). We calculate the number



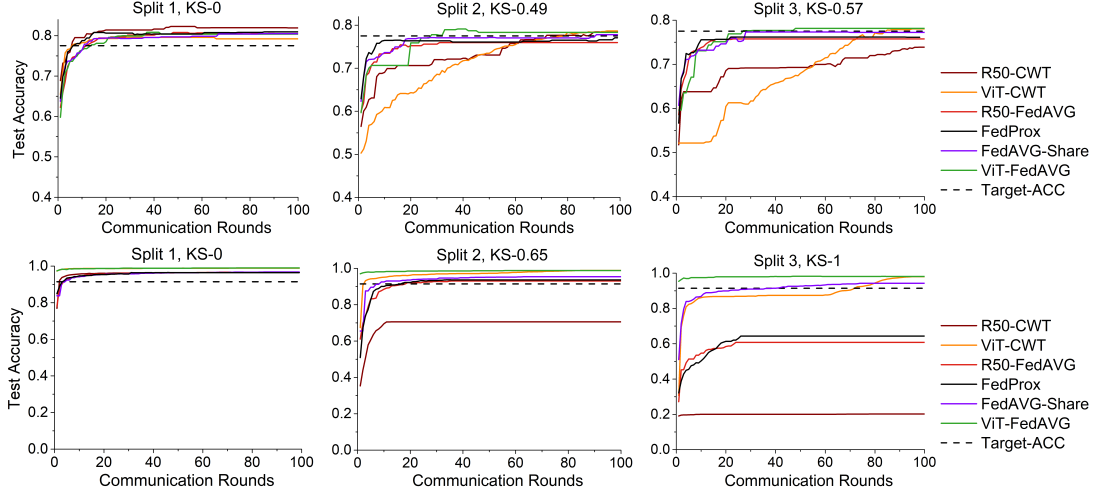


Figure 5: Test set accuracy versus communication rounds on Retina dataset (first row) and CIFAR-10 dataset (second row) with different data partitions. The black dashed line shows the target performance used in Table 3. Vision Transformers converge faster with fewer communication rounds, which make them especially suitable for communication-efficient FL.

	RETINA			CIFAR-10		
	Split-1	Split-2	Split-3	Split-1	Split-2	Split-3
R50-CWT	6	72	$\infty$	2	$\infty$	$\infty$
ViT-CWT	6	79	85	1	3	72
R50-FedAVG	12	$\infty$	$\infty$	4	19	$\infty$
FedProx	7	$\infty$	$\infty$	4	17	$\infty$
FedAVG-Share	11	85	$\infty$	5	9	41
ViT-FedAVG	14	<b>28</b>	<b>27</b>	<b>1</b>	<b>1</b>	<b>1</b>

Table 3: Number of communication rounds needed to reach target performance. Vision Transformers converge faster than existing models especially on increasingly heterogeneous data splits.

of communication rounds needed to achieve a predefined target test set accuracy of 95% of the prediction accuracy of a centrally trained ResNet-50. Specifically, we set the target accuracy of Retina and CIFAR-10 dataset to be 77.5% and 91.5% respectively. We define one communication round on the serial CWT method as one complete training cycle across all federated local clients.

As depicted in Figure 5 and Table 3, all the evaluated FL methods converge to the target test performance quickly on homogeneous data partitions. However, the convergence speed of R50-FedAVG and R50-CWT decrease with increasing heterogeneity and even reach a plateau on highly heterogeneous data partitions (and never reach the target accuracy). In contrast, ViT-FL still converges quickly on heterogeneous data partitions. For example, R50-CWT completely diverges due to severe catastrophic forgetting on heterogeneous data partitions Split-2 and Split-3 on CIFAR-10, whereas ViT-CWT reaches the target performance after 3 and 72 communication rounds. While ViT has more model parameters than ResNet-50 (i.e., 85.8M for ViT-16 and 23.5M for ResNet-50), ViT-FL still reduces total communication costs due to much fewer communication rounds.

#### 4.4 Take-aways for Practical Usage of Transformers in FL

**Local training epochs:** In FL, it is standard to use  $E$  to denote the number of rounds a local model passes over its local dataset.  $E$  is known to strongly affect the performance of FedAVG [43] and CWT [7]. We further conduct an experimental study on the impact of local training epochs  $E$  on ViT-FL to provide guidance for real-world usage. We consider  $E \in \{1, 5, 10\}$  for ViT-FedAVG, and  $E \in \{1, 5\}$  for ViT-CWT. From Figure 6, we find that ViT shows similar phenomena to their CNN counterparts, i.e., larger  $E$  accelerates convergence of ViT-FedAVG on homogeneous data partitions, but may lead to deterioration of final performance on heterogeneous data partitions. Similarly, ViT-CWT also favors frequent transfer rate between each client as R50-CWT [7] on non-IID data partitions.



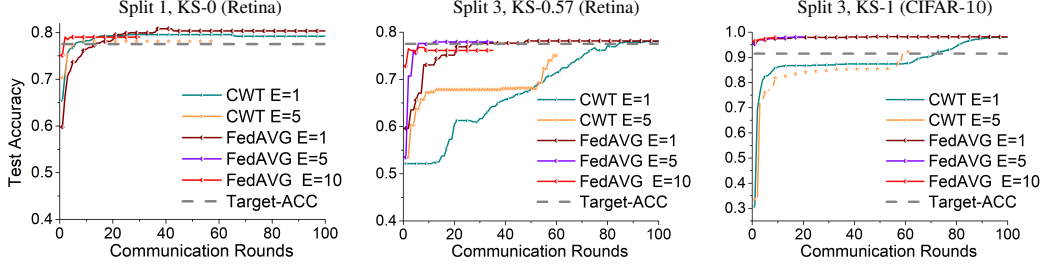


Figure 6: The effect of training over different local epochs  $E$  on each communication round for ViT-CWT and ViT-FedAVG models on Retina and CIFAR-10 dataset (the legend labels CWT and FedAVG and omits the ViT prefix for simplicity). We find that large  $E$  leads to fast convergence in mild heterogeneous data partitions, but might lead to deterioration of the final performance in severely heterogeneous data partitions.

Therefore, we suggest users apply large  $E$  on homogeneous data or mild heterogeneous data partitions to reduce communication cost, but it is recommended to use small  $E$  ( $E \leq 5$  for ViT-FedAVG and  $E = 1$  for CWT) on highly heterogeneous data partitions.

**Other training tips:** Relatively small learning rate and gradient norm clip are necessary to stabilize the training of ViT in CWT, especially in highly heterogeneous data partitions. Gradient norm clip also helps in the training of FL with CNNs across heterogeneous data since it has been shown to reduce weight divergence between local updates and the current global model [33]. Please refer to Appendix B.2 for more general tips and experimental analysis.

## 5 Conclusion

Despite the recent progress in FL, there remain challenges regarding convergence and catastrophic forgetting, especially when dealing with heterogeneous data. Unlike previous methods which focus on improving the optimization process, we provide a new perspective by rethinking architecture design in federated models. Using the robustness of Transformers to heterogeneous data and distribution shifts, we perform extensive experimental analysis and demonstrate the advantages of Transformers in alleviating catastrophic forgetting, accelerating convergence, and reaching a better optimum for both parallel and serial FL methods. We release our code and models to encourage future developments in robust architectures in parallel to current research efforts on the optimization front.

**Limitations:** Despite the promising results of Transformers in FL, several challenges still remain. Firstly, the communication cost is higher than its CNNs counterpart on homogeneous data partitions, as ViT has more communication parameters in each round (larger model size). For heterogeneous data, the communication cost is lower for ViTs, which makes them appealing in this setting (since the number of rounds is reduced due to faster convergence). Therefore, if communication bandwidth is limited, models similar to sparse Transformers [9] could be a sensible alternative. More local training epochs can also be used to reduce communication costs but may deteriorate final performance in heterogeneous data settings. Further analysis of retaining model quality with more local training epochs is an important area for future work. Future work should also adapt Transformers for FL tasks involving image detection and segmentation.

**Broader Impact:** FL provides tools for large-scale distributed training but at the same time requires careful deployment for real-world settings. We outline several potential issues here:

*Privacy:* There may be privacy risks associated with making predictions from sensitive device data. Although federated learning keeps data private on each device without sending it to other locations, it is to reveal private features during distributed model training [6]. Therefore, it remains crucial to obtain user consent before collecting device data and applying it in FL algorithms.

*Security:* Communicating model updates throughout the training process could possibly reveal sensitive information, either to a third party or to the central server [14]. FL could also be sensitive to external security attacks from adversaries [38].

*Fairness:* There can be risks of exposure bias due to imbalanced datasets, especially when personal healthcare data is involved. Models trained on biased data have been shown to amplify the underlying social biases especially when they correlate with the prediction targets [60].

Overall, we believe that our findings can help improve robustness to heterogeneous data and convergence in FL. Future work should further quantify the tradeoffs between performance, communication, privacy, security, and fairness. The flexibility of our approach also offers opportunities for integration with advances in each of these areas, such as differential privacy [10], adversarial training [34], fair representation learning [39], model compression [51], and sequential learning [28].

## References

- [1] Manoj Ghuhana Arivazhagan, Vinay Aggarwal, Aaditya Kumar Singh, and Sunav Choudhary. Federated learning with personalization layers. *arXiv preprint arXiv:1912.00818*, 2019.
- [2] Niranjan Balachandar, Ken Chang, Jayashree Kalpathy-Cramer, and Daniel L Rubin. Accounting for data variability in multi-institutional distributed deep learning for medical imaging. *Journal of the American Medical Informatics Association*, 27(5):700–708, 2020.
- [3] Srinadh Bhojanapalli, Ayan Chakrabarti, Daniel Glasner, Daliang Li, Thomas Unterthiner, and Andreas Veit. Understanding robustness of transformers for image classification. *arXiv preprint arXiv:2103.14586*, 2021.
- [4] Theodora S Brisimi, Ruidi Chen, Theofanie Mela, Alex Olshevsky, Ioannis Ch Paschalidis, and Wei Shi. Federated learning of predictive models from federated electronic health records. *International journal of medical informatics*, 112:59–67, 2018.
- [5] Sebastian Caldas, Sai Meher Karthik Duddu, Peter Wu, Tian Li, Jakub Konečný, H Brendan McMahan, Virginia Smith, and Ameet Talwalkar. Leaf: A benchmark for federated settings. *arXiv preprint arXiv:1812.01097*, 2018.
- [6] Nicholas Carlini, Florian Tramer, Eric Wallace, Matthew Jagielski, Ariel Herbert-Voss, Katherine Lee, Adam Roberts, Tom Brown, Dawn Song, Ulfar Erlingsson, et al. Extracting training data from large language models. *arXiv preprint arXiv:2012.07805*, 2020.
- [7] Ken Chang, Niranjan Balachandar, Carson Lam, Darvin Yi, James Brown, Andrew Beers, Bruce Rosen, Daniel L Rubin, and Jayashree Kalpathy-Cramer. Distributed deep learning networks among institutions for medical imaging. *Journal of the American Medical Informatics Association*, 25(8):945–954, 2018.
- [8] Xinyang Chen, Sinan Wang, Bo Fu, Mingsheng Long, and Jianmin Wang. Catastrophic forgetting meets negative transfer: Batch spectral shrinkage for safe transfer learning. In *NeurIPS*, 2019.
- [9] Rewon Child, Scott Gray, Alec Radford, and Ilya Sutskever. Generating long sequences with sparse transformers. *arXiv preprint arXiv:1904.10509*, 2019.
- [10] Olivia Choudhury, Aris Gkoulalas-Divanis, Theodoros Salonidis, Issa Sylla, Yoonyoung Park, Grace Hsu, and Amar Das. Differential privacy-enabled federated learning for sensitive health data. *arXiv preprint arXiv:1910.02578*, 2019.
- [11] Alexandra Chronopoulou, Christos Baziotis, and Alexandros Potamianos. An embarrassingly simple approach for transfer learning from pretrained language models. In *Proceedings of the 2019 Conference of the North American Chapter of the Association for Computational Linguistics: Human Language Technologies, Volume 1 (Long and Short Papers)*, Minneapolis, Minnesota, June 2019. Association for Computational Linguistics.
- [12] Jacob Devlin, Ming-Wei Chang, Kenton Lee, and Kristina Toutanova. Bert: Pre-training of deep bidirectional transformers for language understanding. *arXiv preprint arXiv:1810.04805*, 2018.
- [13] Alexey Dosovitskiy, Lucas Beyer, Alexander Kolesnikov, Dirk Weissenborn, Xiaohua Zhai, Thomas Unterthiner, Mostafa Dehghani, Matthias Minderer, Georg Heigold, Sylvain Gelly, et al. An image is worth 16x16 words: Transformers for image recognition at scale. In *ICLR*, 2021.
- [14] Jonas Geiping, Hartmut Bauermeister, Hannah Dröge, and Michael Moeller. Inverting gradients—how easy is it to break privacy in federated learning? *arXiv preprint arXiv:2003.14053*, 2020.
- [15] Robert Geirhos, Patricia Rubisch, Claudio Michaelis, Matthias Bethge, Felix A Wichmann, and Wieland Brendel. Imagenet-trained cnns are biased towards texture; increasing shape bias improves accuracy and robustness. *ICLR*, 2019.
- [16] Sharut Gupta, Praveer Singh, Ken Chang, Liangqiong Qu, Mehak Aggarwal, Nishanth Arun, Ashwin Vaswani, Shruti Raghavan, Vibha Agarwal, Mishka Gidwani, et al. Addressing catastrophic forgetting for medical domain expansion. *arXiv preprint arXiv:2103.13511*, 2021.
- [17] Andrew Hard, Kanishka Rao, Rajiv Mathews, Swaroop Ramaswamy, Françoise Beaufays, Sean Augenstein, Hubert Eichner, Chloé Kiddon, and Daniel Ramage. Federated learning for mobile keyboard prediction. *arXiv preprint arXiv:1811.03604*, 2018.

- [18] Kaiming He, Xiangyu Zhang, Shaoqing Ren, and Jian Sun. Deep residual learning for image recognition. In *Proceedings of the IEEE conference on computer vision and pattern recognition*, pages 770–778, 2016.
- [19] Sepp Hochreiter and Jürgen Schmidhuber. Long short-term memory. *Neural Computation*, 9(8):1735–1780, 1997.
- [20] Kevin Hsieh, Amar Phanishayee, Onur Mutlu, and Phillip Gibbons. The non-iid data quagmire of decentralized machine learning. In *International Conference on Machine Learning*, pages 4387–4398. PMLR, 2020.
- [21] Tzu-Ming Harry Hsu, Hang Qi, and Matthew Brown. Measuring the effects of non-identical data distribution for federated visual classification. *arXiv preprint arXiv:1909.06335*, 2019.
- [22] Yen-Chang Hsu, Yen-Cheng Liu, Anita Ramasamy, and Zsolt Kira. Re-evaluating continual learning scenarios: A categorization and case for strong baselines. In *NeurIPS Continual learning Workshop*, 2018.
- [23] Ronghang Hu and Amanpreet Singh. Transformer is all you need: Multimodal multitask learning with a unified transformer. *arXiv preprint arXiv:2102.10772*, 2021.
- [24] Ji Chu Jiang, Burak Kantarci, Sema Oktug, and Tolga Soyata. Federated learning in smart city sensing: Challenges and opportunities. *Sensors*, 20(21):6230, 2020.
- [25] Jason Jo and Yoshua Bengio. Measuring the tendency of cnns to learn surface statistical regularities. *arXiv preprint arXiv:1711.11561*, 2017.
- [26] Kaggle. Diabetic retinopathy detection. <https://www.kaggle.com/c/diabetic-retinopathy-detection>, 2017.
- [27] Peter Kairouz, H Brendan McMahan, Brendan Avent, Aurélien Bellet, Mehdi Bennis, Arjun Nitin Bhagoji, Keith Bonawitz, Zachary Charles, Graham Cormode, Rachel Cummings, et al. Advances and open problems in federated learning. *arXiv preprint arXiv:1912.04977*, 2019.
- [28] James Kirkpatrick, Razvan Pascanu, Neil Rabinowitz, Joel Veness, Guillaume Desjardins, Andrei A Rusu, Kieran Milan, John Quan, Tiago Ramalho, Agnieszka Grabska-Barwinska, et al. Overcoming catastrophic forgetting in neural networks. *Proceedings of the national academy of sciences*, 114(13):3521–3526, 2017.
- [29] Alex Krizhevsky, Geoffrey Hinton, et al. Learning multiple layers of features from tiny images. 2009.
- [30] Siddique Latif, Sara Khalifa, Rajib Rana, and Raja Jurdak. Federated learning for speech emotion recognition applications. In *2020 19th ACM/IEEE International Conference on Information Processing in Sensor Networks (IPSN)*, pages 341–342. IEEE, 2020.
- [31] Yann LeCun, Léon Bottou, Yoshua Bengio, and Patrick Haffner. Gradient-based learning applied to document recognition. *Proceedings of the IEEE*, 86(11):2278–2324, 1998.
- [32] Tian Li, Anit Kumar Sahu, Ameet Talwalkar, and Virginia Smith. Federated learning: Challenges, methods, and future directions. *IEEE Signal Processing Magazine*, 37(3):50–60, 2020.
- [33] Tian Li, Anit Kumar Sahu, Manzil Zaheer, Maziar Sanjabi, Ameet Talwalkar, and Virginia Smith. Federated optimization in heterogeneous networks. *arXiv preprint arXiv:1812.06127*, 2018.
- [34] Paul Pu Liang, Terrance Liu, Liu Ziyin, Nicholas B Allen, Randy P Auerbach, David Brent, Ruslan Salakhutdinov, and Louis-Philippe Morency. Think locally, act globally: Federated learning with local and global representations. *arXiv preprint arXiv:2001.01523*, 2020.
- [35] Tao Lin, Lingjing Kong, Sebastian U Stich, and Martin Jaggi. Ensemble distillation for robust model fusion in federated learning. *arXiv preprint arXiv:2006.07242*, 2020.
- [36] Ziwei Liu, Ping Luo, Xiaogang Wang, and Xiaoou Tang. Deep learning face attributes in the wild. In *Proceedings of the IEEE international conference on computer vision*, pages 3730–3738, 2015.
- [37] Kevin Lu, Aditya Grover, Pieter Abbeel, and Igor Mordatch. Pretrained transformers as universal computation engines. *arXiv preprint arXiv:2103.05247*, 2021.
- [38] Lingjuan Lyu, Han Yu, Jun Zhao, and Qiang Yang. Threats to federated learning. In *Federated Learning*, pages 3–16. Springer, 2020.

- [39] Lingjuan Lyu, Jiangshan Yu, Karthik Nandakumar, Yitong Li, Xingjun Ma, Jiong Jin, Han Yu, and Kee Siong Ng. Towards fair and privacy-preserving federated deep models. *IEEE Transactions on Parallel and Distributed Systems*, 31(11):2524–2541, 2020.
- [40] Kaleel Mahmood, Rigel Mahmood, and Marten Van Dijk. On the robustness of vision transformers to adversarial examples. *arXiv preprint arXiv:2104.02610*, 2021.
- [41] Leland McInnes, John Healy, and James Melville. Umap: Uniform manifold approximation and projection for dimension reduction. *arXiv preprint arXiv:1802.03426*, 2018.
- [42] Brendan McMahan, Eider Moore, Daniel Ramage, Seth Hampson, and Blaise Agüera y Arcas. Communication-efficient learning of deep networks from decentralized data. In *Artificial Intelligence and Statistics*, pages 1273–1282. PMLR, 2017.
- [43] H Brendan McMahan, Eider Moore, Daniel Ramage, Seth Hampson, et al. Communication-efficient learning of deep networks from decentralized data. *arXiv preprint arXiv:1602.05629*, 2016.
- [44] Muzammal Naseer, Kanchana Ranasinghe, Salman Khan, Munawar Hayat, Fahad Shahbaz Khan, and Ming-Hsuan Yang. Intriguing properties of vision transformers, 2021.
- [45] Solmaz Niknam, Harpreet S Dhillon, and Jeffrey H Reed. Federated learning for wireless communications: Motivation, opportunities, and challenges. *IEEE Communications Magazine*, 58(6):46–51, 2020.
- [46] Niki Parmar, Ashish Vaswani, Jakob Uszkoreit, Lukasz Kaiser, Noam Shazeer, Alexander Ku, and Dustin Tran. Image transformer. In *International Conference on Machine Learning*, pages 4055–4064. PMLR, 2018.
- [47] Sayak Paul and Pin-Yu Chen. Vision transformers are robust learners. *arXiv preprint arXiv:2105.07581*, 2021.
- [48] Prajit Ramachandran, Niki Parmar, Ashish Vaswani, Irwan Bello, Anselm Levskaya, and Jonathon Shlens. Stand-alone self-attention in vision models. *NeurIPS*, 2019.
- [49] Nicola Rieke, Jonny Hancox, Wenqi Li, Fausto Milletari, Holger R Roth, Shadi Albarqouni, Spyridon Bakas, Mathieu N Galtier, Bennett A Landman, Klaus Maier-Hein, et al. The future of digital health with federated learning. *NPJ digital medicine*, 3(1):1–7, 2020.
- [50] Holger R Roth, Ken Chang, Praveer Singh, Nir Neumark, Wenqi Li, Vikash Gupta, Sharut Gupta, Liangqiong Qu, Alvin Ihsani, Bernardo C Bizzo, et al. Federated learning for breast density classification: A real-world implementation. In *Domain Adaptation and Representation Transfer, and Distributed and Collaborative Learning*, pages 181–191. Springer, 2020.
- [51] Felix Sattler, Simon Wiedemann, Klaus-Robert Müller, and Wojciech Samek. Robust and communication-efficient federated learning from non-iid data. *IEEE transactions on neural networks and learning systems*, 31(9):3400–3413, 2019.
- [52] Joan Serra, Didac Suris, Marius Miron, and Alexandros Karatzoglou. Overcoming catastrophic forgetting with hard attention to the task. In *International Conference on Machine Learning*, pages 4548–4557. PMLR, 2018.
- [53] Micah J Sheller, Brandon Edwards, G Anthony Reina, Jason Martin, Sarthak Pati, Aikaterini Kotrotsou, Mikhail Milchenko, Weilin Xu, Daniel Marcus, Rivka R Colen, et al. Federated learning in medicine: facilitating multi-institutional collaborations without sharing patient data. *Scientific reports*, 10(1):1–12, 2020.
- [54] Hanul Shin, Jung Kwon Lee, Jaehong Kim, and Jiwon Kim. Continual learning with deep generative replay. *arXiv preprint arXiv:1705.08690*, 2017.
- [55] Yao-Hung Hubert Tsai, Shaojie Bai, Paul Pu Liang, J Zico Kolter, Louis-Philippe Morency, and Ruslan Salakhutdinov. Multimodal transformer for unaligned multimodal language sequences. In *Proceedings of the 57th Annual Meeting of the Association for Computational Linguistics*, pages 6558–6569, 2019.
- [56] Ashish Vaswani, Noam Shazeer, Niki Parmar, Jakob Uszkoreit, Llion Jones, Aidan N Gomez, Łukasz Kaiser, and Illia Polosukhin. Attention is all you need. In *Advances in neural information processing systems*, pages 5998–6008, 2017.
- [57] Praneeth Vepakomma, Otkrist Gupta, Tristan Swedish, and Ramesh Raskar. Split learning for health: Distributed deep learning without sharing raw patient data. *arXiv preprint arXiv:1812.00564*, 2018.

- [58] Haohan Wang, Songwei Ge, Eric P Xing, and Zachary C Lipton. Learning robust global representations by penalizing local predictive power. *NeurIPS*, 2019.
- [59] Hongyi Wang, Mikhail Yurochkin, Yuekai Sun, Dimitris Papailiopoulos, and Yasaman Khazaeni. Federated learning with matched averaging. *arXiv preprint arXiv:2002.06440*, 2020.
- [60] Daniel Yue Zhang, Ziyi Kou, and Dong Wang. Fairfl: A fair federated learning approach to reducing demographic bias in privacy-sensitive classification models. In *2020 IEEE International Conference on Big Data (Big Data)*, pages 1051–1060. IEEE, 2020.
- [61] Michael Zhang, Karan Sapra, Sanja Fidler, Serena Yeung, and Jose M Alvarez. Personalized federated learning with first order model optimization. *ICLR*, 2021.
- [62] Yue Zhao, Meng Li, Liangzhen Lai, Naveen Suda, Damon Civin, and Vikas Chandra. Federated learning with non-iid data. *arXiv preprint arXiv:1806.00582*, 2018.

## Appendix

### A Experimental Details

In this section, we provide additional details on the datasets used, preprocessing steps, and experimental methodology. We include code to reproduce our experiments in a project page at <https://github.com/nips-vit-fl-sub/ViT-FL-main>.

#### A.1 Detailed Image Pre-processing and Data Partitions

**Kaggle Diabetic Retinopathy competition (RETINA)** [26] contains a total of 17,563 pairs of right and left color digital retinal fundus images. Each image is labeled on a scale of 0 to 4 by a well-trained clinician, indicating no, mild, moderate, severe, and proliferative diabetic retinopathy respectively. Following [7], we exclude the samples with scale 1, and then binarize the remaining labels to Healthy (scale 0) and Diseased (scale 2, 3 or 4). Furthermore, we only use the left images in our study to remove the confounding factor of different disease status of left and right eyes for the same patient. We randomly select 6,000 balanced (3,000 healthy and 3,000 diseased) images for training, 3,000 balanced images as the global validation dataset, and 3,000 balanced images as the global test dataset. Other image pre-processing steps include rescaling as a radius of 300, local color averaging and image clipping, resizing to  $256 \times 256$ , horizontal flipping, and randomly cropping to  $224 \times 224$ . We choose a final  $224 \times 224$  image dimension to be compatible with current work in Vision Transformers [13].

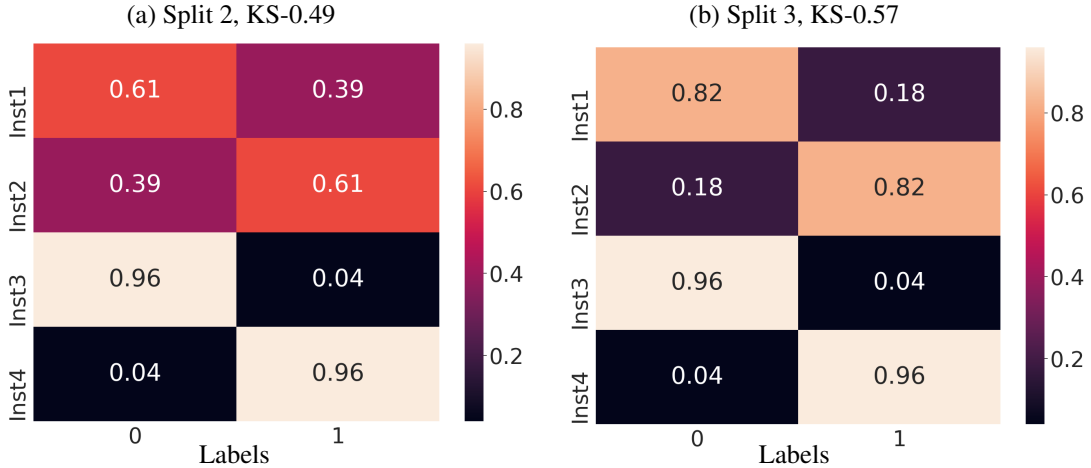


Figure 7: Detailed non-IID data partitions on RETINA with label distribution skew. The value in each rectangle shows the fraction of data samples of a class over their total number.

We simulate three sets of data partitions for the RETINA dataset with each data partition containing four simulated clients: one IID-data partition (Split 1, KS-0), and two non-IID data partitions with label distribution skew (Split 2, KS-0.49, and Split 3, KS-0.57). See Figure 7 for the detailed non-IID data partitions.

**CIFAR-10** CIFAR-10 [29] consists of 50,000 training and 10,000 testing  $32 \times 32$  images in 10 classes, with 5,000 and 1,000 images per class in training and test dataset respectively. Following [20], we apply the 10,000-image test dataset as the global test dataset, set aside 5,000 images from the training dataset as the global validation dataset, and the remaining 45,000 images as training dataset. We preprocess each image by resizing to  $256 \times 256$  and cropping to  $224 \times 224$ .

We simulate one IID-data partition (Split 1, KS-0), one heterogeneous data partition (Split 2, KS-0.65), and one heterogeneous data partition in the extreme case (Split 3, KS-1). Each data partitions contains five clients [7]. We randomly assign each client with images sampled via a uniform distribution over the 10 classes for the IID data partition Split 1, KS-0. For Split 2, KS-0.65, one client receives images sampled from two classes, while the remaining four clients receive images sampled from four classes. Split 3, KS-1 is an extreme case where each client receives images sampled from only two classes. Please refer to Figure 8 for the detailed label distribution on each client for Split 2 and Split 3.



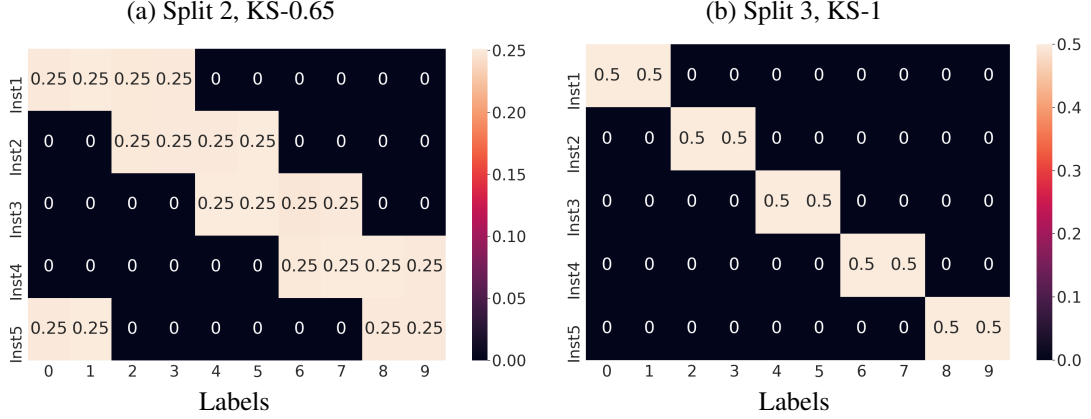


Figure 8: Detailed non-IID data partitions on CIFAR-10 with label distribution skew. The value in each rectangle shows the fraction of data samples in a class over their total number.

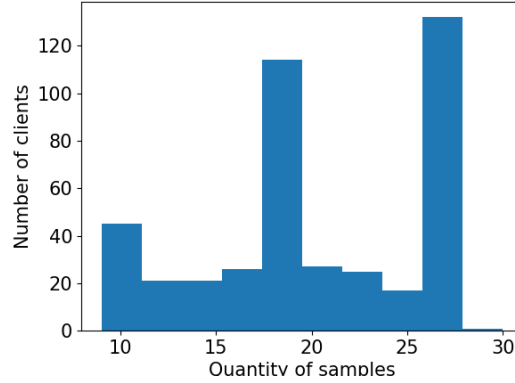


Figure 9: Distribution of samples across clients on the CELEBA dataset.

**CelebA** CELEBA is a large-scale face attributes dataset with more than 200K celebrity images. The images in CelebA cover large diversities, i.e., large pose variations and background clutter. We use a specially designed federated version of CelebA provided by the LEAF benchmark [5] which partitions the dataset into devices based on the celebrity in the picture (i.e., each device contains only images of celebrity). Following [5], we test on the binary classification task (presence of smile), drop clients with fewer than 10 samples, and use 5% of the total clients for training. This results in a total of 429 clients each with an average of  $22.6 \pm 6.23$  samples and a total of 9704 samples, see Figure 9 for the histogram of the number of training samples in each client. We preprocess each image by resizing to  $256 \times 256$  and cropping to  $224 \times 224$ .

## A.2 Implementation Details and Hyperparameters

**Training hyperparameters:** All the methods are implemented with Pytorch and optimized with SGD (with momentum as 0.9 and no weight decay). We set the local training batch size to 32 for all methods except the hybrid (H-ViT) model, where a batchsize of 24 is used due to limited GPU memory. We use learning rate warmup and cosine learning rate decay for all Transformer models. Specifically, we set the warmup steps to 500, and cosine learning rate decay to zero after the maximum round of FL training epochs is reached. The base learning rate is set to 0.03 for the centrally hosted methods and ViT-FedAVG. A smaller learning rate of 0.003 is applied for ViT-CWT methods. The learning rate scheduler for FL with CNNs is selected from linear warm-up and decay or step decay (halved every 30 rounds of FL training).

**Hyperparameter selection:** We tune the best parameters (including learning rate scheduler, momentum parameter  $\beta$  for FedAVGM, and penalty constant  $\mu$  in the proximal term of FedProx) for FL with CNNs on Split-2 of RETINA and CIFAR-10 dataset with grid search, and apply the same parameters

Models	Dataset	Total Round	Warm-steps	LR decay	Base LR	Batch
R50-Central	Retina & CIFAR-10	100	500	cosine	0.03	32
ViT-Central	Retina & CIFAR-10	100	500	cosine	0.03	32
ViT-H-Central	Retina & CIFAR-10	100	500	cosine	0.03	24
R50-CWT	Retina & CIFAR-10	100	500	cosine	0.03	32
R50-FedAVG	Retina & CIFAR-10	100	500	cosine	0.03	32
FedAVGM	Retina	100	0	step	0.03	32
FedAVGM	CIFAR-10	100	500	cosine	0.03	32
FedProx	Retina	100	0	step	0.03	32
FedProx	CIFAR-10	100	500	cosine	0.03	32
FedShare	Retina & CIFAR-10	100	500	cosine	0.03	32
ViT-CWT	Retina & CIFAR-10	100	500	cosine	0.003	32
ViT-FedAVG	Retina & CIFAR-10	100	500	cosine	0.03	32
ViT-H-CWT	Retina & CIFAR-10	100	500	cosine	0.003	24
ViT-H-FedAVG	Retina & CIFAR-10	100	500	cosine	0.03	24

Table 4: Table of hyperparameters for experiments on RETINA and CIFAR-10. All methods are optimized with SGD (momentum 0.9 and no weight decay), and gradient clip at global norm 1. The learning rate is halved every 30 epochs in the step decay scheduler.

Models	Avg. Total Round	Warm-steps	LR decay	Base LR	Batch
R50-Central	30	500	cosine	0.03	32
ViT-Central	30	500	cosine	0.03	32
R50-CWT	30	500	cosine	0.03	32
R50-FedAVG	30	500	cosine	0.03	32
FedProx	30	500	cosine	0.03	32
FedShare	30	500	cosine	0.03	32
ViT-CWT	30	500	cosine	0.003	32
ViT-FedAVG	30	500	cosine	0.03	32

Table 5: Table of hyperparameters for experiments on CELEBA. All methods are optimized with SGD (momentum 0.9 and no weight decay), and gradient clip at global norm 1.

to all the remaining data partitions. The detailed hyperparameters of different models for RETINA and CIFAR-10 are shown in Table 4.

**FL hyperparameters:** For RETINA and CIFAR-10, we set the number of local training epochs  $E$  on each client to 1 (unless otherwise stated) and the total number of communication rounds to 100, with all local clients participating in FL training in each round.  $\beta$  is selected from  $\{0.1, 0.3, 0.5, 0.7, 0.9, 0.97, 0.99, 0.997\}$  for FedAVGM, and is set to 0.5 and 0.3 for Retina and CIFAR-10 dataset, respectively. In FedProx,  $\mu$  is set to 0.001 for Retina dataset and 0.1 for CIFAR-10 dataset by selecting from  $\{0.001, 0.01, 0.1, 1\}$ .

For the CELEBA dataset, we randomly sample 10 clients in each round of FL learning for parallel FL methods. We set  $E$  to 1, the maximum train round to 30 for CWT, and 1000 for all the other parallel FL methods, to ensure each local client joins in FL training for around 30 rounds.  $\mu$  is set to 0.001 for CELEBA dataset. We allow each client to share 5% percentage of their data among each other for FedAVG-Share on all the compared datasets. The detailed hyperparameters are shown in Table 4 and Table 5. Please refer to our project page <https://github.com/nips-vit-fl-sub/ViT-FL-main> for an implementation to reproduce our results.

**Compute:** All experiments were conducted on either a TITAN V GPU or GeForce RTX 2080 GPU.

## B Additional Results

In this section, we provide several additional experimental results that further analyze the effectiveness of Transformers for federated learning.

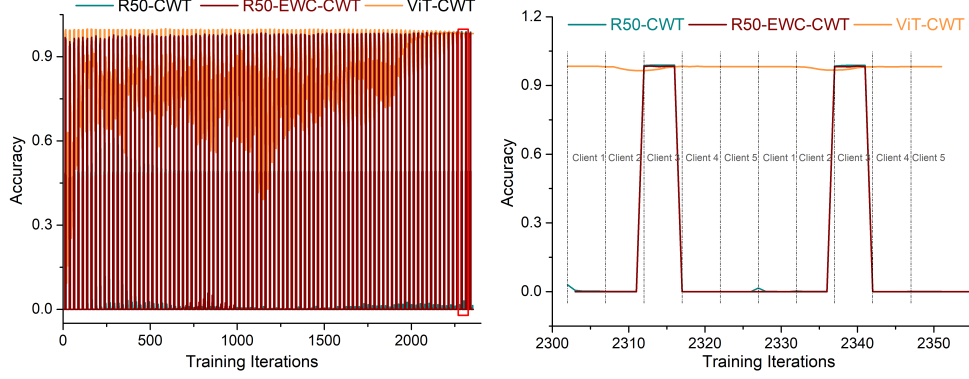


Figure 10: Left: evolution of the prediction accuracy on the validation dataset of client 3 (which shares the same data distribution as its local training dataset) as more clients are involved in CWT learning. We use Split 3 of CIFAR-10 dataset (most heterogeneous data split) and compare the R50-CWT, R50-EWC-CWT, and ViT-CWT models. Right: zoom in on the red rectangular in the left image. The training order of different clients is also shown. EWC barely solves the catastrophic forgetting problem on the highly heterogeneous data partitions, whereas ViT-CWT helps alleviate this problem due to its strong generalization ability and robustness to heterogeneous data.

### B.1 More Comparisons on Catastrophic Forgetting

We further compare ViT-CWT with an optimization method specifically designed to alleviate catastrophic forgetting, elastic weight consolidation (EWC) [28], on Split-3 of CIFAR-10 data. We use the implementation from [22] for EWC and test it with the same experimental setting reported in Section 4.3.1. The serial training of CWT on Split-3 of CIFAR-10 can be considered as an incremental class learning task where each client contains an exclusive subset of classes in the dataset. Each client model shares the same classifier to a standardized union label space [22]. As depicted in Figure 10, EWC barely solves the catastrophic forgetting problem on the highly heterogeneous data partitions, which also matches the results reported in [22]. This experiment further demonstrates the effectiveness of ViT beyond optimization methods specially designed for FL.

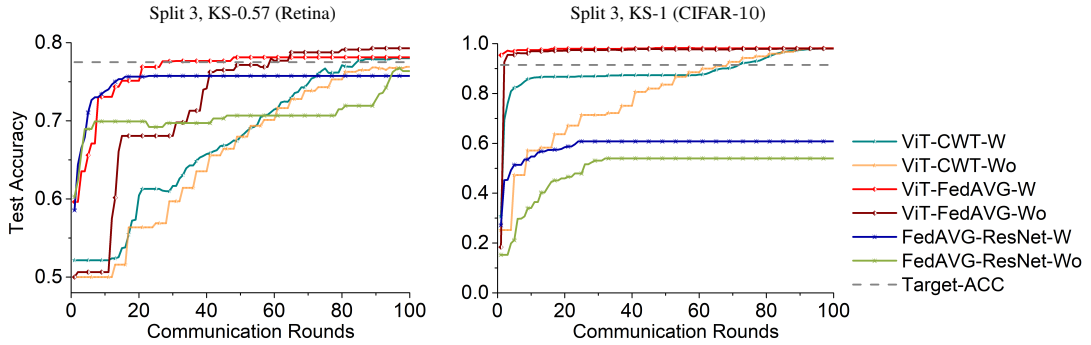


Figure 11: Influence of gradient clip on different FL methods. In the legend, **-W** denotes with gradient clip and **-Wo** denotes without gradient clip. We find that gradient clip stabilizes training and accelerates convergence speed on highly heterogeneous data splits.

### B.2 Take-aways for Practical Usage

The training strategy of ViT in FL can be directly inherited from ViT training, such as using linear warm-up and learning rate decay, and gradient clip. We also notice that gradient clip stabilizes training for most FL methods on the highly heterogeneous data partition, and therefore can be applied as a general technique in FL applications (see Figure 11 of ViT-FL and R50-FedAVG with and without gradient clip). The training of ViT-CWT favors a relatively smaller learning rate on heterogeneous data partitions, whereas using a smaller learning rate for CNN counterparts leads

	RETINA			CIFAR-10		
	Split-1	Split-2	Split-3	Split-1	Split-2	Split-3
R50-CWT (GN)	82.21	81.13	77.05	95.10	93.87	87.70
R50-FedAVG (GN)	82.40	80.13	80.57	96.39	95.12	86.20

Table 6: Prediction accuracy (%) of CWT and FedAVG on RETINA and CIFAR-10 when using ResNet50 (GN) as the backbone network. Replacing the batch normalization layer with group normalization in ResNet50 still suffers performance loss on highly heterogeneous data partitions, indicating that the promising performance of ViT-FL does not come purely from not using batch normalization.

to worse performance. In real-world applications, users can use a large learning rate for IID or mild-skewed data partitions for ViT-CWT, but a smaller learning rate is necessary to stabilize training for highly heterogeneous data partitions.

### B.3 Investigating the Influence of Normalization Technique in ViT-FL

The batch normalization layer has been shown to be one of the major factors that deteriorate the performance of federated learning methods on non-IID data partitions [20, 16]. Hsieh *et al.* [20] demonstrate that group normalization (or layer normalization) can avoid the skew-induced accuracy loss of batch normalization on non-IID data. This may raise the question: does the promising performance of ViT-FL come purely from not using a batch normalization layer? To answer this question, we compare ViT-FL with FL-ResNet50 (GN) by replacing all batch normalization layers in ResNet-50 with group normalization. As shown in Table 6, group normalization indeed helps to obtain better performance for both CWT and FedAVG on mildly skewed data partitions than their batch normalization counterparts. For example, the performance on Split-2 of CIFAR-10 is improved from original 70.58% (see R50-CWT in Table 2) to 93.87%. However, it still suffers performance loss on highly skewed data partitions. In contrast, ViT-FL consistently shows promising results on both mildly skewed and extremely highly skewed data partitions, indicating that the effectiveness ViT-FL does not arise purely from different normalization techniques.